Journal of Power Sources 196 (2011) 6003–6006

Contents lists available at ScienceDirect

Journal of Power Sources

journal homepage: www.elsevier.com/locate/jpowsour

Short communication

KOH modified graphene nanosheets for supercapacitor electrodes

Yueming Li [a], Marshall van Zijll [b], Shirley Chiang [b], Ning Pan [a,*]

[a] Nanomaterials in the Environment, Agriculture, and Technology (NEAT), University of California at Davis, CA 95616, United States
[b] Department of physics, University of California at Davis, CA 95616, United States

ARTICLE INFO

Article history:
Received 14 January 2011
Received in revised form 22 February 2011
Accepted 22 February 2011
Available online 6 March 2011

Keywords:
Graphene
Modification
Supercapacitor

ABSTRACT

Chemical modification of graphene nanosheets by KOH was examined as a way to enhance the specific capacity of graphene nanosheets in supercapacitor. Fourier transform infrared spectroscopy, Raman spectroscopy and X-ray photoelectron spectroscopy were used to investigate the effects of the treatment on the surface of the graphene nanosheets. The specific capacitance of 136 F g^{-1} was obtained for KOH treated graphene by integration of the cyclic voltammogram, an increase of about 35% compared with that for the pristine graphene nanosheets.

1. Introduction

In recent years, electrochemical supercapacitors (ECs) have drawn increasing attentions in the filed of electrochemical energy storage and conversion owing to their high power capability and long cycle-life [1,2]. Generally, on the basis of the energy storage mechanism, supercapacitors establish capacitance via two ways. The capacitance owing to pure electrostatic charge accumulated at the electrode/electrolyte interface is called the electric double-layer capacitance (EDLC), while the capacitance due to a Faradaic process is named as pseudocapacitance. The capacitance and energy density both are strongly dependent of the electrode materials used in the supercapacitor, and so far activated carbons are mostly studied and have been commercially used in EDLC typed supercapacitor. However, there is an increasing demand for supercapacitors as power storage device with higher energy density. To satisfy this demand, it is crucial to explore new materials with large capacitance. There have been a lot of efforts to develop novel carbon based materials for supercapacitor such as carbon nanotubes [3–6], carbon aerogels [7,8] and mesoporous carbon [9,10]. Although these carbon materials have shown good electrochemical performance as EDLC materials, their complicated preparation process and high costs restricted the practical uses in large scale [11].

Graphene nanosheets, as new type of carbon with two-dimensional nanostructure, have attracted escalating attention due to their unique properties such as the quantum hall effect at room temperature [12]. They are also considered as appealing candidate electrode materials in energy storage field due to their good electrical conductivity, low cost, excellent mechanical property and high specific surface area. Recently many reports demonstrated that graphene nanosheets [13–16] and their composites such as MnO_2/graphene [17], polyaniline/graphene [18], $Ni(OH)_2$/graphene [19] possessed a high capacity as electrode materials in supercapacitor. Certain chemical modification of graphene nanosheets might help to further improve the electrochemical performance [20,21]. Although the specific capacitance of the carbon materials can be greatly increased after activation with KOH [11,22], the approach has not been reported on chemical activation of graphene nanosheets.

Here, we report the modification of the graphene nanosheets using concentrated KOH solution and their resulted electrochemical performance as supercapacitor electrode materials. The primary electrochemical experiments showed that the specific capacitance was greatly enhanced after such modification.

2. Experimental

2.1. Materials and methods

All chemicals were of analytical grade and used without further purification. Double distilled de-ionized water was used for making all the solutions. In a typical experiment, 1.5 g graphene nanosheet powders (XG sciences) were added to 150 mL KOH (10 M) aqueous solution, ultrasonic for 3 h. Then the mixture solution was washed and filtered with distilled water until the pH of filtrate water became neutral. The filtered product was dried at 100 °C for 12 h.

* Corresponding author. Tel.: +1 530 752 6232; fax: +1 530 752 7584.
E-mail address: npan@ucdavis.edu (N. Pan).

0378-7753/$ – see front matter © 2011 Elsevier B.V. All rights reserved.
doi:10.1016/j.jpowsour.2011.02.092

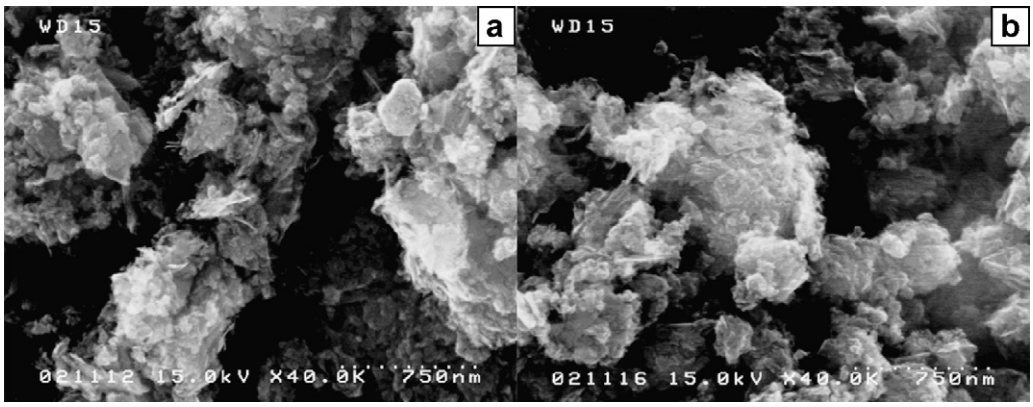

Fig. 1. SEM images of pristine graphene nanosheets (A) and KOH treated graphene nanosheets (B).

2.2. Characterization

Fourier transform infrared (FT-IR) spectra of the samples were carried out on a Thermal Micolet 6700 within the range of 1000–2000 cm^{-1} using KBr pellet. The scanning electron microscope (SEM) images were recorded using a Hitachi 4100 FE scanning electron microscope. The Raman spectrum was carried out on a Renishaw Raman spectrum (514 nm excitation) in the range of 1000–3000 cm^{-1}. X-ray photoelectron spectra (XPS) were carried out in the advanced surface microscopy facility with an X-ray photoelectron spectrometer. N_2 adsorption/desorption isotherms were obtained by a gas adsorption analyzer (ASAP2020, Micromeritics Instrument Co.) at 77 K.

2.3. Electrochemical characterization

The KOH modified graphene electrodes were prepared as follows. The modified graphene powders were mixed with carboxymethyl cellulose as a binder in a weight ratio of 90:10, and then the mixture was incorporated onto a nickel foam (1.0 cm × 10 cm). The pasted nickel electrodes were dried at 80 °C under vacuum and then pressed at a pressure of 5 MPa for 1 min. For comparison, as-purchased pristine graphene powder electrode was also prepared using the same procedures as described above.

The cyclic voltammetry (CV) measurements and electrochemical impedance spectroscopy (EIS) were carried out on a Princeton 263A electrochemical workstation (Princeton Applied Research, USA) at room temperature. The experiments were carried out in a three-electrode glass cell in which the as prepared electrode acted as the working electrode, graphite as the counter electrode (surface areas of about 5 cm^2), and Ag/AgCl in saturated KCl aqueous solution as the reference electrode, along with 1 M Na_2SO_4 aqueous solution as the electrolyte.

3. Results and discussion

Field-emission scanning electron microscope was used to examine the morphology of KOH modified graphene powders. The SEM images of both the pristine graphene powder and KOH modified graphene powders are shown in Fig. 1A and B, respectively. The pristine graphene powders are composed of aggregated sheets closely associated with each other as judged from the photos. After treated by KOH, the morphology showed no obvious changes compared with that of the pristine graphene, i.e., the treatment exerted little effect on the internal structure.

The surface functional groups of graphene and modified graphene particles were studied by FT-IR. As shown in Fig. 2A, two new peaks appeared after KOH modification in comparison to that of the pristine graphene powders. The peaks around 1385 cm^{-1} can be assigned to the deformation vibrations of an H–C–OH group [23] whereas the peak at 1632 cm^{-1} as well as a small peak at 1680 cm^{-1} is the characteristic of the $-COO^-$ vibration [24]. These new peaks proved that some oxygen-containing groups were introduced on the edges of graphene during the treatment.

Fig. 2B is the Raman spectrum of the pristine and KOH modified graphene nanosheets. The peak at 1345 cm^{-1} (D band) is caused by the defects and disorders in the hexagonal graphitic layers while the peak at about 1570 cm^{-1} (G band) corresponding to an E_{2g} mode of graphite is related to the vibration of sp^2-bonded carbon atoms in a two-dimensional hexagonal lattice. The intensity of D-band

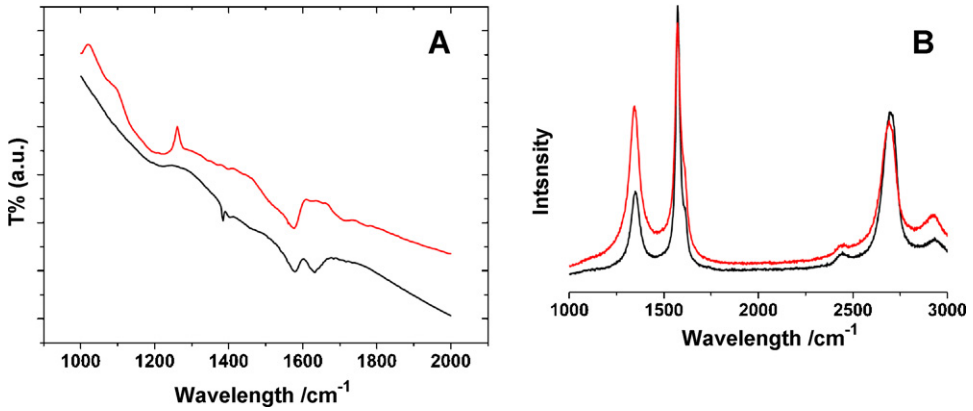

Fig. 2. FT-IR (A) and Raman (B) spectrum of pristine graphene (red line) and KOH treated graphene nanosheets (black line). (For interpretation of the references to color in this figure legend, the reader is referred to the web version of the article.)

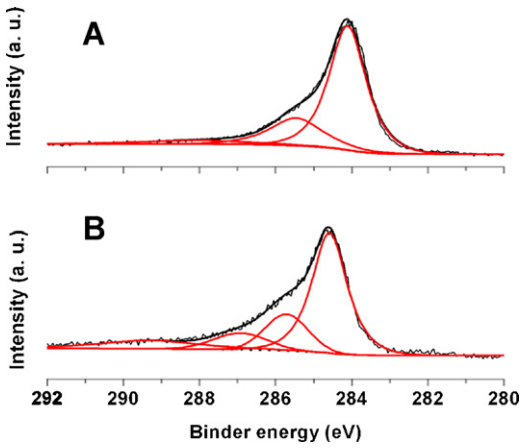

Fig. 3. XPS spectrum of pristine graphene (A) and KOH treated graphene nanosheets (B).

decreased and that of G-band increased after modification, suggesting that the treatment led to edge defects (rather than basal defects), removal of amorphous carbon and ash and increase of graphitic character [25–27].

XPS was used to reveal the nature of carbon and oxygen bond in the pristine and KOH treated graphene nanosheets. Their C1*s* spectra of both samples (Fig. 3) are asymmetric, suggesting that both samples contain some amounts of oxygen-containing surface groups. The C1*s* spectrum of pristine graphene nanosheets (Fig. 3A) shows two main components at a BE (binding energy) of 284.1 and 285.5 eV, which are due to the presence of graphitic carbon and C–OH on the surface pristine graphene sheets, respectively [28]. After KOH treatment, two new components at 286.9 and 289.3 eV (corresponding to C=O and (C=O)–O groups, respectively) plus the original two components were clearly observed (shown in Fig. 3B), indicating the introduction of oxygen-containing functional groups to graphene nanosheets [29].

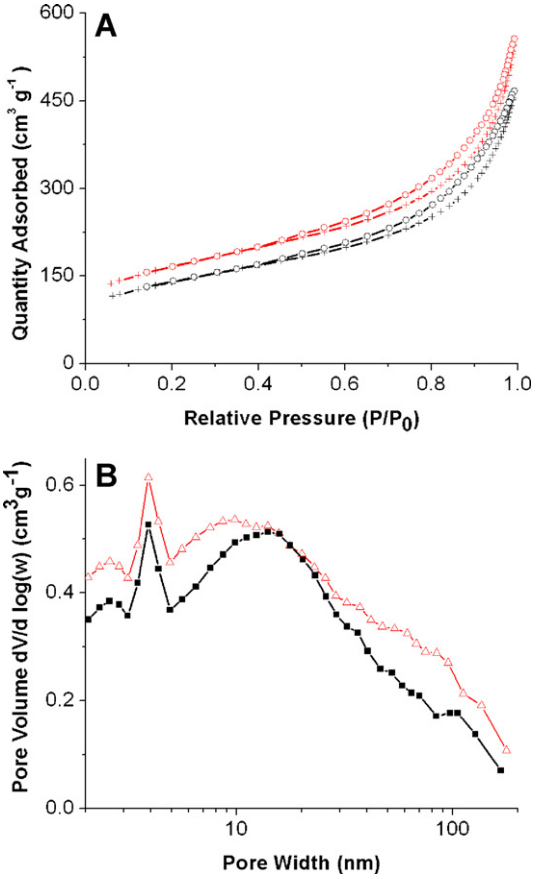

Fig. 4. N_2 adsorption–desorption isotherms (A); pore size distributions of the untreated (red)/treated (black) graphene nanosheets (B). (For interpretation of the references to color in this figure legend, the reader is referred to the web version of the article.)

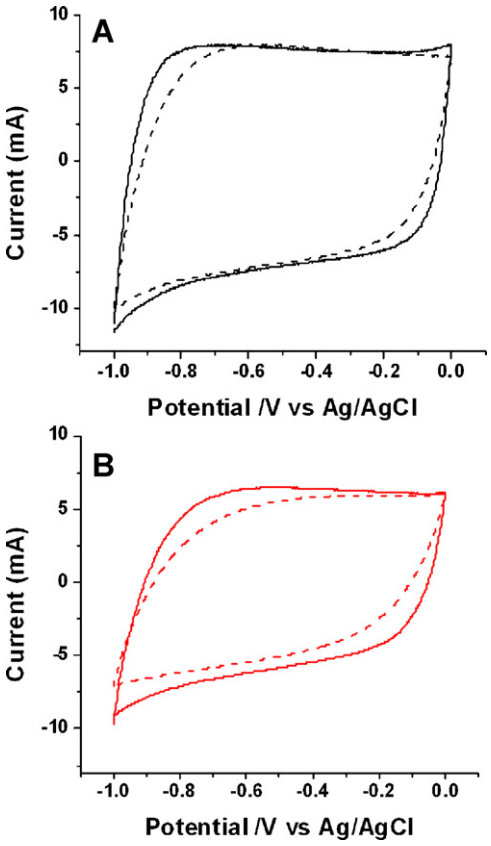

Fig. 5. Cyclic voltammogram of KOH treated graphene nanosheets (a), and pristine graphene nanosheets (b); (solid line 10 mV s^{-1}; dash line 20 mV s^{-1}).

N_2 adorption measurements were carried out to determine their surface areas and pore-size distribution. Fig. 4 presents the N_2 adsorption isotherms of the treated/untreated graphene nanosheets together with the corresponding pore-size distributions. The isotherms of both samples exhibit type III characteristics, indicating broad size-distribution of pore sizes extending into the large mesopore and/or macropore range. The pore-size distributions from the adsorption branch of the isotherms using the Barrett, Joyner and Halenda (BJH) method reveal the broad distribution of mesopores from 2 to 100 nm for both samples. The KOH modified graphene nanosheets exhibited a Brunauer–Emmett–Teller (BET) surface area of 492 m^2 g^{-1}, decreased a little compared with that of untreated sample (584 m^2 g^{-1}). The decrease was likely caused due to the blocking of the pores by the surface functional groups introduced via KOH treatment [30].

The typical cyclic voltammogram is shown in Fig. 5. As is shown, the CV curves have a more rectangular shape for the treated graphene, suggesting an improved capacitive behavior. The specific capacitance of the graphene nanosheets electrode is calculated using the integrated area of the charge curve [4]. The pristine graphene sheets only exhibited a specific capacitance of 101 F g^{-1} (corresponding to 14.0 W h kg^{-1} in energy density *E*, according to $E = CV^2/2$) while the KOH modified graphene sheets resulted in a specific capacitance of 136 F g^{-1} (corresponding to 18.9 W h kg^{-1}

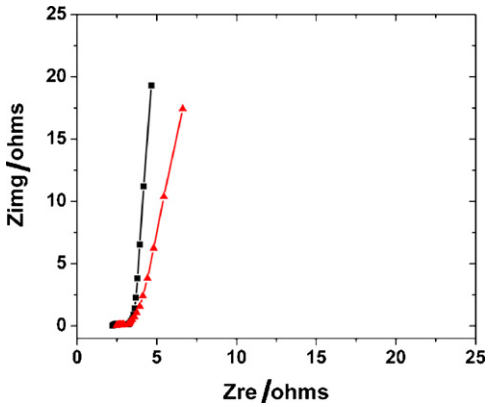

Fig. 6. EIS curve of pristine graphene sheets (red line) and KOH treated graphene nanosheets (black line). (For interpretation of the references to color in this figure legend, the reader is referred to the web version of the article.)

in energy density) at the scan rate of 10 mV s^{-1}. In other words, the specific capacitance increased about 35% after modification. With the increase of the scanning speed to 20 mV s^{-1}, the specific capacitance of treated graphene nanosheets (123 F g^{-1}) is also higher than that of the pristine graphene nanosheets (81 F g^{-1}). These experiments showed that the electrochemical performance was significantly improved by the KOH treatment. The increased capacity might be related to the edge defects and the oxygen-containing groups introduced by the KOH modification, which not only increases the accessibility of the graphene nanosheets by the electrolyte, but also leads to further pseudocapacitive effects [31]. Also, compared with the conventional KOH modification to other carbon materials which requires high temperature and inert gas protection, this method is simple and more cost-effective [22].

In Fig. 6, the Nyquist plot of both graphene electrodes shows a straight line in the low-frequency region and a small semicircle in the high frequency region. The intersection of the curve with the *X*-axis represents the internal or equivalent series resistance (ESR) which is a key parameter in influencing the charge/discharge rate, as a smaller ESR value represents a lesser internal loss and a greater charge/discharge rate. As seen from the curve, the ESR value reduced after treated with KOH, indicating a decreased internal resistance. The vertical shape at lower frequencies indicates a pure capacitive behavior, representative of the ion diffusion in the structure of the electrode [32]. The curve become more vertical after treatment with KOH, suggesting the KOH treated electrode behaves more closely to an ideal capacitor than the pristine electrode. The more rectangular CV curves and more vertical EIS spectra for modified graphene might be related to the removal of amorphous carbon and ash in the pristine graphene nanosheets under ultrasonic and KOH solution [27].

4. Conclusion

We reported in this study the KOH modified graphene nanosheets and their performance as supercapacitor electrode materials. The edge defects and oxygen containing groups have been resulted in the treated graphene powders. The KOH treated graphene as electrode materials were characterized and tested, and yielded enhanced specific capacitance value over the untreated graphene. This method might provide a simple and more cost-effective route to improve the electrochemical performance of graphene powders as supercapacitor electrode materials.

Acknowledgement

This work was supported by the grant of California EISG 55697A/07-21.

References

[1] J.R. Miller, P. Simon, Science 321 (2008) 651.
[2] M. Winter, R.J. Brodd, Chem. Rev. 104 (2004) 4245.
[3] C.M. Niu, E.K. Sichel, R. Hoch, D. Moy, H. Tennent, App. Phys. Lett. 70 (1997) 1480.
[4] K.H. An, W.S. Kim, Y.S. Park, Y.C. Choi, S.M. Lee, D.C. Chung, D.J. Bae, S.C. Lim, Y.H. Lee, Adv. Mater. 13 (2001) 497.
[5] C. Emmenegger, P. Mauron, P. Sudan, P. Wenger, V. Hermann, R. Gallay, A. Zuttel, J. Power Sources 124 (2003) 321.
[6] T. Bordjiba, M. Mohamedi, L.H. Dao, Adv. Mater. 20 (2008) 815.
[7] R. Saliger, U. Fischer, C. Herta, J. Fricke, J. Non-Cryst. Solids 225 (1998) 81–85.
[8] H. Probstle, M. Wiener, J. Fricke, J. Porous Mater. 10 (2003) 213.
[9] A.B. Fuertes, G. Lota, T.A. Centeno, E. Frackowiak, Electrochim. Acta 50 (2005) 2799.
[10] C.O. Ania, V. Khomenko, E. Raymundo-Pinero, J.B. Parra, F. Beguin, Adv. Funct. Mater. 17 (2007) 1828.
[11] E. Frackowiak, Phys. Chem. Chem. Phys. 9 (2007) 1774.
[12] K.S. Novoselov, A.K. Geim, S.V. Morozov, D. Jiang, Y. Zhang, S.V. Dubonos, I.V. Grigorieva, A.A. Firsov, Science 306 (2004) 666.
[13] M.D. Stoller, S.J. Park, Y.W. Zhu, J.H. An, R.S. Ruoff, Nano Lett. 8 (2008) 3498.
[14] X. Zhao, H. Tian, M.Y. Zhu, K. Tian, J.J. Wang, F.Y. Kang, R.A. Outlaw, J. Power Sources 194 (2009) 1208.
[15] R. Louie, MRS Bull. 33 (2008) 1133.
[16] Y. Wang, Z.Q. Shi, Y. Huang, Y.F. Ma, C.Y. Wang, M.M. Chen, Y.S. Chen, J. Phys. Chem. C 113 (2009) 13103.
[17] Q.L. Du, M.B. Zheng, L.F. Zhang, Y.W. Wang, J.H. Chen, L.P. Xue, W.J. Dai, G.B. Ji, J.M. Cao, Electrochim. Acta 55 (2010) 3897.
[18] K. Zhang, L.L. Zhang, X.S. Zhao, J.S. Wu, Chem. Mater. 22 (2010) 1392.
[19] H.L. Wang, H.S. Casalongue, Y.Y. Liang, H.J. Dai, J. Am. Chem. Soc. 132 (2010) 7472.
[20] M.H. Liang, L.J. Zhi, J. Mater. Chem. 19 (2009) 5871.
[21] T. Cassagneau, J.H. Fendler, Adv. Mater. 10 (1998) 877.
[22] A. Kuznetsova, D.B. Mawhinney, V. Naumenko, J.T. Yates, J. Liu, R.E. Smalley, Chem. Phys. Lett. 321 (2000) 292.
[23] G.X. Zhu, X.W. Wei, S. Jiang, J. Mater. Chem. 17 (2007) 2301.
[24] Y. EinEli, V.R. Koch, J. Electrochem. Soc. 144 (1997) 2968.
[25] S. De, P.J. King, M. Lotya, A. O'Neill, E.M. Doherty, Y. Hernandez, G.S. Duesberg, J.N. Coleman, Small 6 (2010) 458.
[26] A.C. Ferrari, J.C. Meyer, V. Scardaci, C. Casiraghi, M. Lazzeri, F. Mauri, S. Piscanec, D. Jiang, K.S. Novoselov, S. Roth, A.K. Geim, Phys. Rev. Lett. 97 (2006) 187401.
[27] A. Rinaldi, B. Frank, D.S. Su, S. Bee, A. Hamid, R. Schlgöl, Chem. Mater. 23 (2011) 926.
[28] S. Park, J.H. An, R.D. Piner, I. Jung, D.X. Yang, A. Velamakanni, S.T. Nguyen, R.S. Ruoff, Chem. Mater. 20 (2008) 6592.
[29] S. Yumitori, J. Mater. Sci. 35 (2000) 139.
[30] J.W. Shim, S.J. Park, S.K. Ryu, Carbon 39 (2001) 1635.
[31] A.G. Pandolfo, A.F. Hollenkamp, J. Power Sources 157 (2006) 11.
[32] W.C. Chen, T.C. Wen, H.S. Teng, Electrochim. Acta 48 (2003) 641.